Swinburne Astronomy Online AST80018
Time Assignment Submission
Bayer Group Submission Form

M31: Metallicity Gradient of LMXBs

.

:		

1. General summary of science justification and expected outcomes – (written for public consumption).

[Limit of 1 page including any figures or tables. Minimum acceptable font size is 11 point]

Stars very often come in pairs called binaries, and each of the individuals in a binary system can be at very a different stage of their evolution. An X-ray binary star system is one in which a compact neutron star (or black hole) is accreting matter from its near-by companion which is usually a hydrogen-fusing, main sequence star. The stars are so close that, for systems with a companion up to one solar mass (Low Mass X-ray Binary-LMXB), their gravitational boundaries overlap and material is drawn from the companion star, through the intersection space and onto an accretion disk around the massive, but physically smaller, host star. The companion in these systems are cooler than spectral Class A. As material flows towards the accretion disk of the host, it is heated to millions of degrees and emits brightly in X-ray, although the system is visually dim because of the developmental stage of the companion.

Where there are many stars in close proximity to each other, the chances are greatly increased for a binary of this nature to form. One of the places where these conditions exist is in Globular Clusters (GC) and particularly in their highly dense cores. GCs are spherical balls of around a million stars that generally inhabit the halo of late type galaxies, although recent studies show that they have a much more complex distribution, evolution and range of morphologies. Generally thought to have a common origin, the stars in a GC are well evolved but have low concentrations of elements heavier than hydrogen (low metallicity). LMXBs develop 100 times more often in GCs than in the general star field, and this formation has a poorly understood relationship to metallicity.

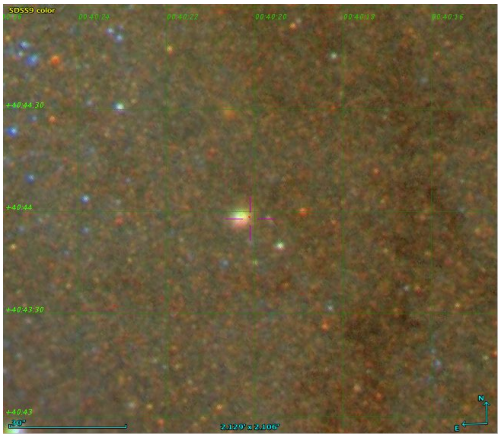

Globular cluster 2E 114 is a bright visual and X-ray source in Andromeda galaxy

Galaxy formation and the role of GCs in their evolution is an active area of research in astronomy. It is difficult to understand how GCs and host galaxies evolve by studying the Milky Way (MW) from within, but we have a nearby laboratory in the Andromeda galaxy (M31). Albeit twice the width and containing three times as many stars as the MW, it originated at a similar cosmic time and has similarly grown by cannibalising other galaxies. It also has a population of GCs.

Due to ongoing studies, the state of the population of GCs within M31 is somewhat complicated by competing theories of galactic evolution, galactic collisions and stellar streams. Depending on author and definition, there are at least several hundred bona fide GCs within M31, and probably as many again in nearby gravitational attachments. It is a dynamic system under much scrutiny.

Studying the relationships between GC mass, metallicity, LMXBs and distribution can constrain our theories of galaxy evolution and so observing these immensely powerful X-ray beacons in space is an important scientific pursuit. We intend this to be the first of a series of observations that will allow us to accumulate GC LMXB metallicity data for targets with a large range of radial distances from the centre of M31, allowing us to "*...disentangle contributing variables*…", as suggested in the literature (Agar, J. & Barmby, P. 2013, AJ, 146, 5, id. 135).

2. Scientific Justification.

[Limit of 3 pages, including any images, tables and reference list. Minimum acceptable font size is 11 point]

Early theory of how LMXBs formed is by dynamic interaction such as the tidal capture of a star (Fabian et al. 1975) or direct collision of the bodies (Sutantyo et al. 1975; Peacock et al. 2009). These early works were based on observations within the MW, indicating that GCs were a major source of LMXBs (Clark 1975). The GCs contained more LMXBs than would be expected based on their masses alone (Peacock et al. 2009). Studies of GCs within the MW are hampered due to dust within the galactic plane and a low number of GCs. With the development of new technologies, studies of LMXBs extended to intergalactic space. The advent of Chandra, XMM-Newton and ROSAT telescopes have made it possible to observe extragalactic sources.

Several studies of LMXBs and their parameters have been conducted and this telescope time application relates to obtaining data of the metallicity gradient of LMXB GCs as they vary in distance from the galactic centre of M31. Bellazzini et al. (1995) reviewed X-ray data of M31 and the MW obtained from Einstein and ROSAT space telescopes and determined that bright LMXB sources ($L > 10^{36}$ ergs/s) are generally denser than non-X-ray GCs and are also of higher metallicity. It is claimed that a metallicity dependence on the Initial Mass Function (IMF) (the Salpeter slope) could increase the frequency of LMXBs irrespective of the actual mechanism of the LMXB's formation.

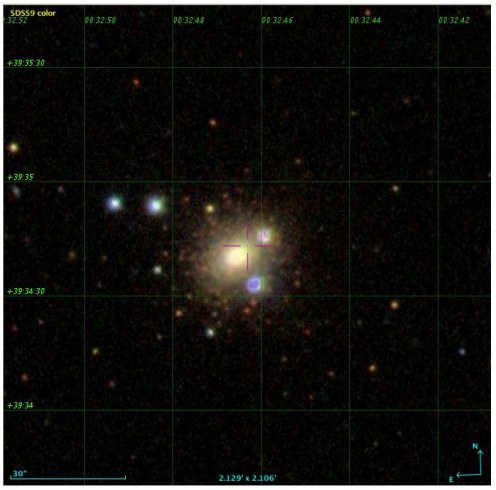

GC Mayall II is a very weak X-ray source in M31's halo.

Trudolyubov & Priedhorsky's (2004) review of data from XMM-Newton and Chandra observatories confirmed Bellazzini et al. (1995) report that M31's inferred X-ray luminosity (L_x) of GC is in the order of ~10^{35} to 10^{39} erg/s and that the brighter GCs in M31 are optically brighter and more metal-rich than non-X-ray GCs and tend to be at a greater distance from the centre. However for luminosities above 10^{38} erg/s the LMXBs tended to reside in metal-poor GCs. A comprehensive study carried out by Peacock et al. (2010) of LMXBs in M31 based on further data from XMM-Newton and Chandra identified strong connections between the presence of LMXBs and metallicity, luminosity and stellar collision rates.

van den Bergh (1969) claimed that there was no evidence of a correlation between metallicity and radii. However a subsequent analysis of reddening, colour and metallicity by Fan et al. (2008) showed that there was a correlation between metallicity and radii from the galactic centre and evidence of a metallicity gradient for metal-poor GCs but no such indication for metal-rich GCs. There was a distribution of CGs at varying radii with metal-rich GC more centrally located while metal-poor GCs were more widely spaced with decreasing metallicity at increasing radius. The study did not make a differentiation between LMXBs and non-X-ray GCs, a position this requested telescope time will address.

Vulic et al (2016) observed 259 new X-ray sources between 0.5-8.0 keV and L_x of ~10^{34} erg/s citing an aging population of LMXBs in the bulge. Haghi et al. (2017) compares the stellar Mass–to-Light (M/L) Ratio of M31 GCs and their metallicity [Fe/H] with Strader et al.'s (2011) determination of the kinematics and structural properties and M/L ratios of 163 GCs in M31. The Strader et al. (2011) results were based on the optical (V band) and near infrared (K band). Haghi et al. (2017) consider the results are not borne out by observations and propose that if the IMF is taken into account, a better correlation with observations is

achieved. Haghi et al. (2017) developed an age-metallicity relationship (AMR) and took into account the IMF and the metallicity, which compares more favorably with observations.

As indicated above there have been several studies carried out on generally metallicity of GCs and on LMXBs and the relationship between them. Some are contentious. LMXBs appear to be dependent not only on metallicity and its gradient but also on the IMF, age and location about the galactic centre. No specific study has been carried out into the metallicity gradient of LMXB GCs.

The question to be addressed in this proposal is whether metallicity is a major factor in the formation and evolution of GCs containing LMXBs and if so, is this factor a function of distance from the galactic centre. Peacock et al. (2009) has shown a relationship between the presence of LMXB and mass and collision rates as one mechanism for forming binaries. Though metallicity derivations from X-ray spectra are contentious (eg Kapferer et al 2007, Pintore & Zampieri 2011), and we expect very low photon counts, the spectra obtained from our observations will provide data that can be used in modeling the presence of LMXBs in GCs generally, and go some way towards understanding the relationship, if any, between GC metallicity and their distance from galactic cores.

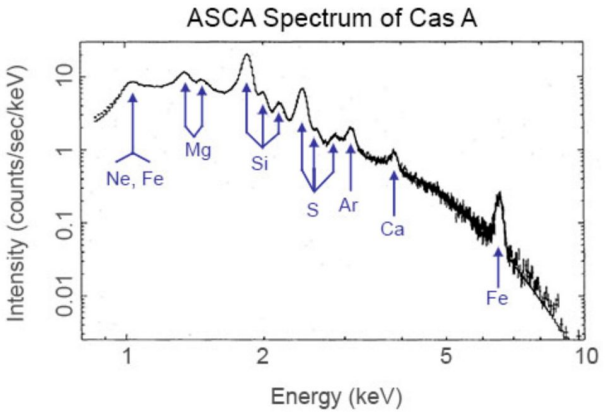

X-ray spectrum of supernova remnant Cas A from ASCA data. (Credit: Holt et al., PASJ 1994)

The graph on the right shows an X-ray spectrum from a SNR with metal emission lines indicated. We are hoping to reduce data received from NuSTAR observations so as to quantify similar lines. Surveys of X-ray sources within M31's GCs have been limited. Maccarone et al. (2016) discovered three likely X-ray binaries when observing the brightest ($L_X \sim 10^{38}$ erg/s) X-ray sources within M31's GCs for ~ 100 ks. Given the success of Wik et al. (2016) at detecting fainter and hence possibly LMXB sources within M31 and that of Maccarone et al. (2016) in detecting X-ray binaries within M31 GCs, we are confident of detecting LMXBs within most of our selected GCs.

M31 Astrometrics (NEDweb)

Name: M31 (Andromeda, NGC 224) is a SA(s)b LINER galaxy
Distance: 0.784 Mpc (σ = 0.121)
Heliocentric radial velocity: -300 km/s (± 4)
Magnitude: 4.36
Equatorial (J2000.0) coordinates:
[Deg.: 10.6847929 + 41.269065] [hh:mm:s: 00:42:44.3503 +41:16:08.634 ± 8.00e-02]

NuSTAR Details (NuSTARweb)

NuSTAR is able to resolve bright X-ray binaries (i.e. with an L_X on the order of several 10^{38} erg/s) up to 4 Mpc away. This is well within M31's distance meaning that 120 less luminous X-ray binaries (down to a L_X less than 10^{37} erg/s) within the disk and bulge of M31 have been successfully detected in the 4-25 keV band with 1 Ms in total exposure time using NuSTAR (Wik et al. 2016).

The images below give a sense of the visible and corresponding X-ray environments around five of our targets.

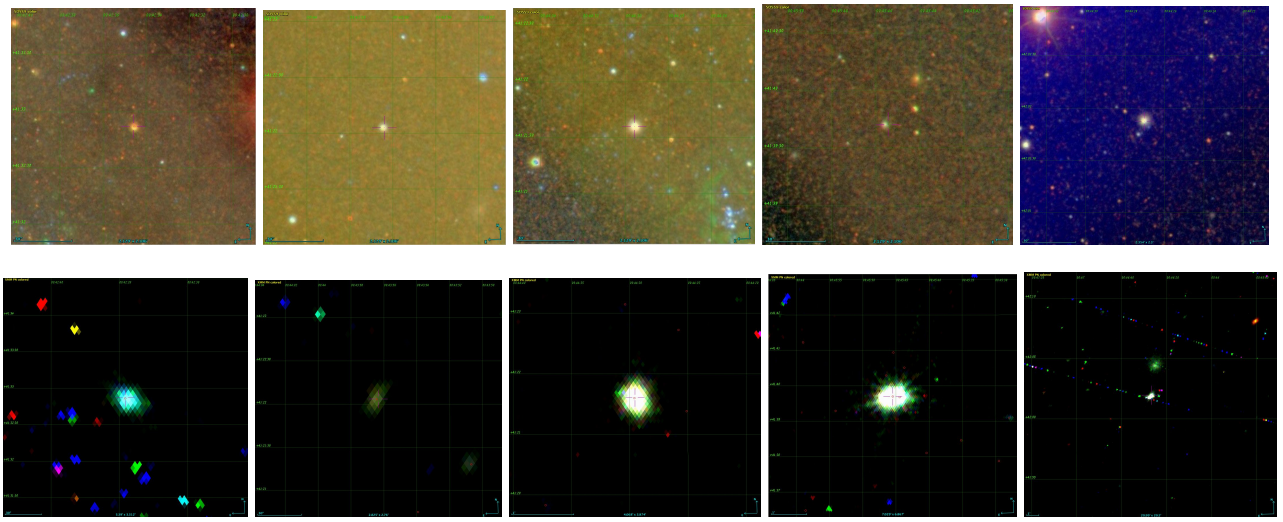

2E 146 2MASS J00435642+4122027 2E 166 2E 169 BA 3-8

Visible (top row) and X-ray sources that correlate closely with GCs. From left to right, they are 0.04, 0.30, 0.44, 0.76 and 0.93 degrees from the core of M31 (Credit: CDS Aladin,SDSS, XMM)

References

Bellazzini, M. et al., 1995, ApJ, 1, 439, 2, 687
Clark, G. W. 1975, ApJ, 199, pt 2, L143
Fabian, A. C. et al., 1975, MNRAS, 172, 15
Fan, Z. et al. 2008, MNRAS, 385, 1973
Haghi, H. et al., 2017, ApJ, 839, 1, id. 60
Harrison, F. A. et al., 2013, ApJ, 770, 2, 103
Kapferer, W., et al., 2007, arXiv:0707.1573
Maccarone, T.J. et al., 2016, MNRAS, 458, 3633
NCCweb: NuSTAR Science Operations Center - Check Constraints Page, http://www.srl.caltech.edu/NuSTAR_Public/NuSTAROperationSite/CheckConstraint.php (accessed 19 Oct 2017)
NEDweb: NASA/IPAC Extragalactic Database, http://ned.ipac.caltech.edu/cgi-bin/objsearch?objname=m31&extend=no&hconst=73&omegam=0.27&omegav=0.73&corr_z=1&out_csys=Equatorial&out_equinox=J2000.0&obj_sort=RA+or+Longitude&of=pre_text&zv_breaker=30000.0&list_limit=5&img_stamp=YES (accessed 1 Nov 2017)
ObsGuideweb: NuSTAR Guest Observer Program Observatory Guide, https://heasarc.gsfc.nasa.gov/docs/nustar/nustar_obsguide.pdf (accessed 19 Oct 2017)
Peacock, M. B. et al., 2009, MNRASL, 392, 1, L55
Peacock, M. B. et al., 2010, MNRAS, 407, 4, 2611
Pintore, F. & Zampieri, L. 2011, MNRAS, 420, 2, 1107
Strader, J. et al., 2011, ApJ, 142, 1, id. 8
Sutantyo, W. 1975, A&A, 44, 227
Trudolyubov, S. & Priedhorsky, W. 2004, ApJ, 616, 821
van den Bergh, S. 1969, ApJS, 19, 145
VizieRweb: VizieR web pages, http://vizier.u-strasbg.fr/viz-bin/VizieR-2 (accessed 1 Nov 2017)
Vulic, N. et al, 2016, MNRAS, 461, 4, 3443
Watson, M. G. *et al.*, 2009, A&A, 493, 339
Wik, D.R. et al. 2016, American Astronomical Society, HEAD meeting #15, id.402.02

3. Technical Justification and Observing Details

[Limit of 1 page including any images, tables. Minimum acceptable font size is 11 point]

For guest observers, NuSTAR allows a maximum exposure time per observation of 500 ks (just under 139 hours) (ObsGuideweb). This will allow us to observe fainter X-ray sources than observed by Maccarone et al. (2016), although not quite as faint as those detected by Wik et al. (2016).

Just over 4 hours integration times are sufficient to sample a spectrum (Harrison et al. 2013) and CCD detector response is close to tested values - at energies below 50 keV, resolution is 0.4 keV FWHM. Above 50 keV, charge trapping in the CCD broaden the FWHM to 1.9 keV for 86 keV photons.

Four hours observing each target plus up to 24 hours to slew between targets requires an allowance of 28 hours per target. We have 139 hours, so we list seven (7) targets (chosen from Watson, M. G. *et al.*, 2009 and 2XMMi-Newton catalogue) in order of preference. Our request is the first of six applications for similar observing sessions so that spectra for at least 30 GCs are obtained.

The online NuSTAR constraints calculator (NCCweb) confirms that for observing M31 in the current evaluated period (01 Jun 2017 - 31 May 2018) there are Sun-aspect and tracker-visibility violations which restrict us to the following observation dates:

- 01 Jan - 20 Jan (~480 hrs)
- 01 Feb - 03 Feb (~72 hrs)
- 13 Feb - 19 Feb (~168 hrs)
- 23 Feb - 04 Mar (~240 hrs)
- 13 Mar - 15 Mar (~72 hrs)
- 10 May - 25 May (~384 hrs)

Team Bayer will be happy to accept NuSTAR scheduling in any of these periods.

Previously recorded ranges in flux for requested targets (VizieRweb)

The expected fluxes are difficult to predict as some are variable and there are some discrepancies in the literature. Our seven targets have been observed previously in the 0.2 - 12 keV band, by several telescopes, and the values below have been distilled from contributors to the VizieR database:

	Dimmest to Brightest (mW/m^2)	Brightest ($erg/cm^2/s$) for camera (M1, M2)
1. B386-G322 (GC BA 3-8)	(6.38828e-17) - (2.99894e-15)	(5.6887e-15 M1)
2. B375-G307 (GC 2E 169)	(1.82346e-13) - (9.63260e-12)	(1.1144e-11 M1)
3. B225-G280 (GC 2E 166)	(4.54071e-14) - (1.61434e-12)	(1.7809e-12 M1)
4. B204-G254 (GC 2MASS J00435642+4122027)	(3.22232e-15) - (8.58533e-14)	(1.6196e-13 M2)
5. B116-G178 (GC 2E 146)	(2.35266e-15) - (7.70434e-13)	(9.015e-13 M2)
6. B005-G052 (GC 2E 114)	(5.16819e-14) - (3.47300e-12)	(3.80e-12 M2)
7. G001-MII (GC Mayall II)	(8.99622e-16) - (2.44610e-14)	(2.72e-14 M1)

4. Technical justification and Observing details.

This may include, but is not limited to: telescope, instrument, filters needed, number of nights required, phase of moon, preferred dates, etc.

[Limit of 1 page including any images and tables. Minimum acceptable font size is 11 point]

The literature contains a number of observations of our requested targets, all with slightly different astrometric data, so we list here their approximate positions, and links to the SIMBAD and VizieR data bases.

Requested targets and their SIMBAD data

1. B386-G322 (GC BA 3-8)..... SIMBAD data. Edge of visual disk
2. B375-G307 (GC 2E 169)..... SIMBAD data. On disk edge
3. B225-G280 (GC 2E 166)..... SIMBAD data. Outer part of disk?
4. B204-G254 (GC 2MASS J00435642+4122027)..... SIMBAD data. Half way out disk?
5. B116-G178 (GC 2E 146)..... SIMBAD data. ⅔ way out disk?
6. B005-G052 (GC 2E 114)..... SIMBAD data. ½ way out disk?
7. G001-MII (GC Mayall II)..... SIMBAD data. VERY dim x-ray in halo

Requested targets and their VizieR data

	Target	RA (Dec. ^{o})	Dec (Dec. ^{0})	L_x (10^35 erg/s)	Distance to M31 (Deg.)	VizieR Link
1.	B386-G322	11.612469	+42.031350	1573.8	0.93…….	2XMMi J004626.9+415429
2.	B375-G307	11.439532	+41.661614	7013.5	0.76…….	2XMMi J004545.4+413941
3.	B225-G280	11.123257	+41.360027	1175.4	0.44……..	2XMMi J004429.5+412136
4.	B204-G254	10.985118	+41.367648	62.5	0.30……..	2XMM J004356.3+412203
5.	B116-G178	10.644032	+41.547694	561.0	0.04……..	2XMMi J004234.5+413251
6.	B005-G052	10.083819	+40.732910	2528.7	0.60……..	2XMM J004020.1+404358
7.	G001-MII	8.194110	+39.577931	17.0	2.50……..	2XMM J003246.5+393440

5. Object details (please modify or extend this table as appropriate, so that all relevant information on chosen observing targets is included).

Depending on realised slew rates and settling times, we request up to seven (7) observations within the allotted 500ks. Observations may have more than one GC in the FoV (as below) but we have specified the targets of interest within each FoV. For NuSTAR convenience, the object details below are *ordered sequentially from largest RA and priority*. Except for the first and last objects, we have selected targets with bright X-ray fluxes and which do not have large visual offsets. Details of the objects in each FoV and our targets (listed first in blue) are here:

FoV 1:

- **BA 3-8** (Lx = 1573.8 x 10^35 erg/s) (0.93° from M31) very bright at edge of M31
  (hh:mm:s 00:46:27.02 +42:01:52.7) (Deg. 0.7741722222 +42.03130556)

FoV 2:

- **2E 169** (Lx = 7013.5 x 10^35 erg/s) (0.76° from M31) very bright
  (hh:mm:s 00:45:45.577 +41:39:42.25) (Deg. 0.7626583333 +41.66173611)
- SK182C Lx = 143 x 10^35 erg/s 0.78° from M31 large visual offset

FoV 3:

- **2E 166** (Lx = 1175 x 10^35 erg/s) (0.44° from M31) very bright
  (hh:mm:s 00:44:29.483 +41:21:35.56) (Deg. 0.7415222222 +41.35987778)
- SK091C Lx = 5.7 x 10^35 erg/s 0.45° from M31 faint

FoV 4:

- **2MASS J00435642+4122027** (Lx = 62.5 x 10^35 erg/s) (0.30° from M31) bright
  (hh:mm:s 00:43:56.43 +41:22:02.8) (Deg. 0.7323416667 +41.36744444)
- B182-G233 Lx = 57.2 x 10^35 erg/s 0.22° from M31 bright
- B050-G113 Lx = 31.4 x 10^35 erg/s 0.24° from M31
- B193-G244 Lx = 52.8 x 10^35 erg/s 0.25° from M31 bright
- B035 Lx = 14.2 x 10^35 erg/s 0.30° from M31 faint

FoV 5:

- **2E 146** (Lx = 561.0 x 10^35 erg/s) (0.04° from M31) bright
  (hh:mm:s 00:42:34.544 +41:32:51.4) (Deg. 0.7095944 +41.5476111)
- BH18 Lx = 6 x 10^35 erg/s 0.02° from M31 large visual offset, faint
- B117-G176 Lx = 14.2 x 10^35 erg/s 0.04° from M31 faint
- B107-G169 Lx = 231.6 x 10^35 erg/s 0.06° from M31 large visual offset, bright
- B098 Lx = 16.3 x 10^35 erg/s 0.07° from M31 faint
- B096-G158 Lx = 106.2 x 10^35 erg/s 0.08° from M31 large visual offset, bright
- B159 Lx = 13.5 x 10^35 erg/s 0.13° from M31 large visual offset, faint
- B161-G215 Lx = 16.2 x 10^35 erg/s 0.13° from M31 faint

FoV 6:

- **2E 114** (Lx = 2528.7 x 10^35 erg/s) (0.60° from M31) very bright
  (hh:mm:s 00:40:20.32 +40:43:58.3) (Deg. 0.6723111111 +40.73286111)

FoV 7:

- **Mayall II** (Lx = 17.8 x 10^35 erg/s) (2.5° from M31) VERY dim x-ray in halo
  (hh:mm:s 00:32:46.53 +39:34:40.5) (Deg. 0.5462583333 +39.57791667)